Romanian Reports in Physics, Vol. 65, No. 3, P. 1052–1062, 2013

Dedicated to Professor Valentin I. Vlad's 70th Anniversary

MANIFESTATIONS OF LINEAR DICHROISM CHANGES IN CANCER BIOTISSUES

A. ANGELSKAYA[1], I. GRUIA[2], S. YERMOLENKO[1], P. IVASHKO[1], M. GRUIA[3]

[1] Chernivtsi National University, Correlation Optics Dept., 2 Kotsjubinsky Str., 58012 Chernivtsi, Ukraine, E-mail: angelsky@itf.cv.ua
[2]University of Bucharest, Faculty of Physics, Sector 5, 36-46 Mihail Kogalniceanu Blvd, 050107 Bucharest, Romania, E-mail: gruia_ion@yahoo.com
[3]Oncologic Institute "Al. Trestioreanu", Sos. Fundeni nr. 252, Sector 2, Bucharest, Romania, Email: gmariaiuliana@yahoo.com

Received June 14, 2013

Abstract. The anisotropic properties of the cancerous tissue's slices by polarimetry and spectropolarimetry methods are studied. We combine optical and biochemical techniques for identification of the cell membrane transformation in the dynamic of growth and development of experimental solid tumour. It is shown that in all cases the linear dichroism appears in biological tissues (the human esophagus, the muscle tissue of rats, mice's melanoma, prostate tissue) with a cancer disease, the magnitude of which depends on the type of tissue and on duration of the cancer process development.

Key words: polarization, biotissue, malignant tumor, spectropolarimetry, dichroism.

1. INTRODUCTION

The malignant transformation of normal cell is not a rare event, considering that any cell in the normal cycle division has the potential to become malignant. However, most people go through life without a cancer, detecting and control of the body are able to stop the cells to be transformed in tumours. Although malignant tumour cells take birth in normal cells, morphology of them is much changed from the cells of origin. Optical microscopy studies have allowed to shape characteristics of cellular abnormalities. Biological membranes play a crucial role in all cellular phenomena.

Major progress made in biological and biochemical studies of biological membranes is that they are not static entities with rigid structures [1, 2]. Maintaining the structure of liquid crystal, both lipids and proteins have freedom of movement. Flow can be regarded as disorderly movement of individual

carbohydrate chains of molecules double layer. Mobility and rigidity of protein and lipid molecules are favoured by temperature and high degree of unsaturated carbohydrate links and the length of carbohydrate chains. Decreased fluidity can be observed experimentally by lowering the temperature. If a high percentage of fat molecules in the membrane are unsaturated, the melting temperature membrane is lower than body temperature. In this way a part of the double layer is fluid, and the polar groups of lipid molecules can move freely.

After the malignant transformation, the cytoplasm membrane is the first modified structure [3, 4]. Early detection of malignant transformation is a goal of modern medicine and to this end there is an impressive number of approaches from the scientific field that tries to identify early changes preceding malignant transformation in order to establish correct diagnosis.

This paper aims to combine the optical and biochemical techniques for identifying the changes in membrane dynamics of growth and development of experimental solid tumours.

2. MATERIALS AND TECHNIQUES FOR BIOCHEMICAL STUDIES

Tumours obtained in murine models are considered experimental and currently an important tool in elucidation of the malignant mechanisms, there is no perfect model for clinical oncology. Transplanted tumours in animal experience are different from human tumours in several respects: the rate of growth is much faster, less heterogeneous cell is expressed, develop-invasive and infiltration capacity have much lower metastasis. A major disadvantage of transplanted tumours is the appearance of subpopulations with differentiated cell biological behaviour from parental cells.

Despite these many shortcomings, murine tumours transplanted in conjunction with in vitro models (cell culture, tissue and organs) continue to support the biological basis for various cancer studies. Walker 256 carcinosarcoma is a standard used tumour in the preclinical screening of antibodies, as well as in various experimental models of chemo-radio-immunotherapy. Percentage of holding a subcutaneous tumour grafts is 80–90%. In Wistar rats the metastasis are rare, and the invasion of loco-regional nodes occurs in the terminal phase of tumour growth when tumour necrosis phenomena are emphasized (Figs. 1–4).

Researches were conducted on male Wistar rats with average weight of 110 g, clinically healthy, from the animal house of the Institute of Oncology from Bucharest. Tumoral implant was performed with a suspension of cells, about 1×10^7 cells in 1.0 ml saline buffer subcutaneous injection in the right flank. At 7 days after the cells inoculation the first clinical manifestations appears, tumour was tangible after 14 days [5, 6].

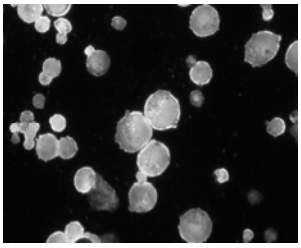

Fig. 1 – Walker cells – with acridine orange colour; ×20 objective.

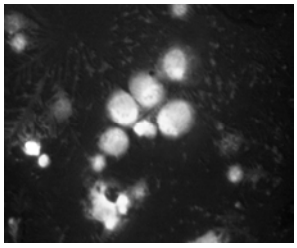

Fig. 2 – Walker cells – with acridine orange colour; ×20 objective. DNA fluorescent green-yellow, red RNA fluorescence.

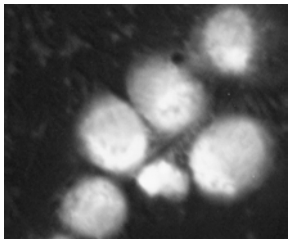

Fig. 3 – Walker cells – with acridine orange colour: DNA fluorescent green-yellow, red RNA fluorescence flame red or claret.

Tumoral volume for each tumour is calculated in part by the relationship:

$$V_{tumoral} = a \times b^2 \times 0.52, \quad (1)$$

where: a – large diameter of tumour (mm); b – diameter of small tumour (mm); tegument thickness – 0.52 (mm).

2.1. PREPARATION OF BIOLOGICAL SAMPLES

Blood was collected by cardiac puncture (without anticoagulant), centrifuge at 3 000 rpm for 15 minutes. The serum was used for analysis. After taking each sample tumoral tissue and the liver were obtained homogeneous tissues grown by grinding with saline (at 1 g of tissue were added 10 ml saline). After centrifugation at 3 000 rpm was used for analysis serum.

Determination of lipid peroxides was performed in serum, tissue and tumoral liver tissue. Determination of thiol groups was performed in tissue and tumoral liver tissue.

2.2. RESULTS AND DISCUSSIONS

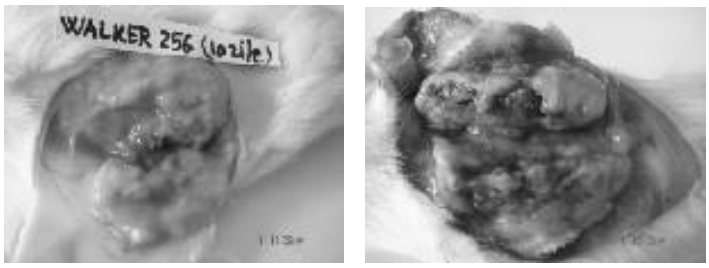

Fig. 4 – Walker carcinoma 256.

The tumour is well vascularise with dilated vessels near the numerous outbreaks of necrosis. Lipid Peroxidation is a classic example of the radicals mechanism chained reaction. Although the auto oxidation or lipids peroxidation under the action of reactive oxygen species is a widely accepted phenomenon, mechanisms and consequences of its interpretation is very controversial due to the great diversification. This can be explained by the composition of extremely varied quality and quantity of lipids in polyunsaturated fatty acids by different experimental conditions. Lipid peroxides were assessed by measuring the concentration of MDA, the end product of lipid degradation.

Table 1

	14 days	17 days	24 days
Ser	6.07µmol/100ml	9.74µmol/100ml	7.83µmol/100ml
Peritumoral tissue	4µmol/100 ml	5.26µmol/100ml	6.19µmol/100ml
Tumoral tissue	7.76µmol/100ml	9.91µmol/100ml	7.93µmol/100ml

Action of active oxygen metabolites in the structural proteins or enzymes cause distortion thereof. In most frequent interactions occur also in thiol groups of proteins which in turn may undergo oxidation or exposure of thiol groups of proteins is essential. This explains the increased sensitivity to oxidation of denatured proteins (this property is used as an effective method of identifying content in these groups and to identify secondary and tertiary structure of proteins). Total albuminic thiol groups were determined by react ion with acid-5.5`ditio-bis (2-nitrobenzoic) (Elman reagent), DTNB noted.

Table 2

	14 days	17 days	24 days
Ser	566 µmol /l	215 µmol /l	104 µmol /l
Peritumoral tissue	640 µmol /l	540 µmol /l	218 µmol /l
Tumoral tissue	701 µmol /l	495 µmol /l	344 µmol /l

Oxidative stress may be defined as a dynamic imbalance between the production in excess of reactive oxygen species to the detriment of their capture and neutralization of the endogenous antioxidant systems. When installed, oxidative stress may be reversible and is a production of free radicals in excess, but for a shorter period, or when action is irreversible for a long time, the concentration of free radicals and the higher effects are disastrous for the integrity and functioning of cell.

3. LASER POLARIMETRY OF OPTICALLY THICK BIOLOGICAL TISSUES

For estimation of diagnostic potentialities of statistical analysis of the prostate tissue images, the histological sections of physiologically normal (21 samples) and oncologically changed (22 samples) of the tissue were investigated.

For carrying out such study, a new installation has been created, which optical scheme [7] is shown in Fig. 5.

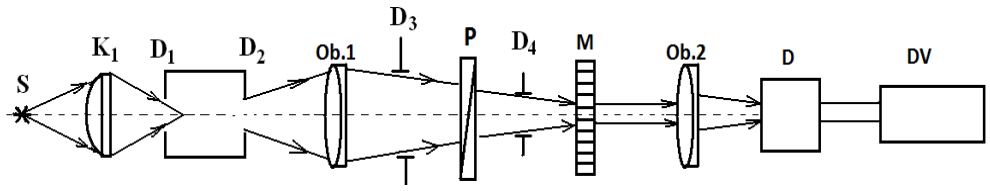

Fig. 5 – Optical setup.

Here: S – a stabilized source of radiation; K1 – a lighted condenser; D1 and D2 – an entrance and exit slot of the monochromator MUM; Ob.1 and Ob.2 – objectives; D3 and D4 – diaphragms; P – a polarizer, Nicol prism; M – an investigated sample; D – radiation detector: in the domain λ = 330÷600 nm – photomultiplier, in the domain λ = 600÷750 nm – the silicon photodiode FD-24K; DV – digital voltmeter.

Sample M is fixed in limb and can be rotated in the beam from 0^o to 360^o the plane of polarization of light after the polarizer P. This makes it possible to determine the minimum bandwidth (in the dominant orientation elements of the sample parallel to the plane of polarization) – τ_0 and maximum bandwidth (in the dominant orientation elements of the structure of the sample perpendicular to the plane of polarization) – τ_{90} for each given wavelength λ after monochromator. To obtain the absolute magnitudes of transmittance in the direct beam, a sample is derived from the zone of the beam – a digital voltmeter registers the magnitude of the normalization signal I_0.

Polarization images of optically thin (reduction factor $\tau \le 0.1$, geometrical thickness is 40 μm) histological sections of healthy (a, b) prostate tissue and oncologically changed (c, d) one obtained for coaxial (0-0) and crossed (0-90) polarizer 4 and analyzer 9 are presented in Fig. 6.

The analysis of the obtained results showed high diagnostic sensitivity of statistic moments of the 3rd and 4th orders of coordinate distributions of matrix elements of both types of biological tissues to the changes of optical-geometric structure.

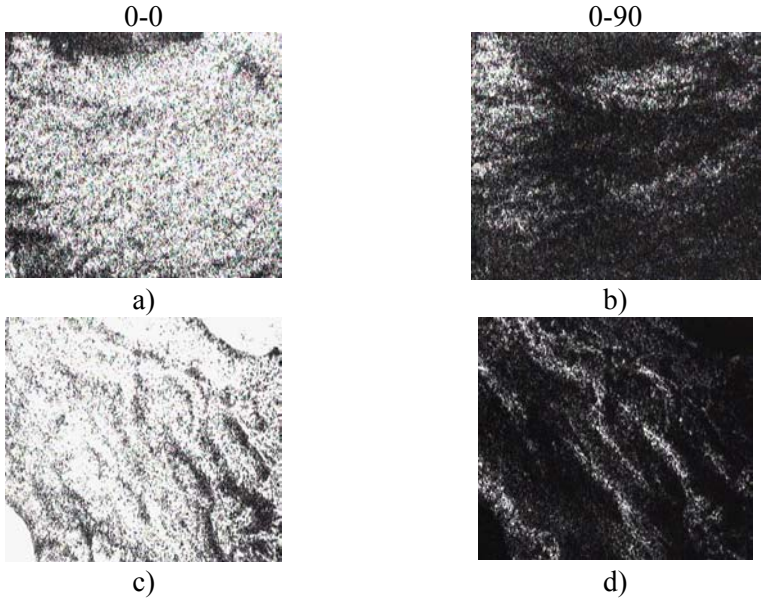

Fig. 6 – Polarization images of the healthy (a, b), and oncologically changed (c, d) prostate tissues.

4. LINEAR DICROISM OF BIOLOGICAL TISSUES OF DIFFERENT TYPES

In biophysical photometry, the convenient technique for determining optical properties of objects and environments (absorption coefficient, optical density) at which measurements are made in a narrowly focused beam is used rarely. This is because virtually all biological objects (leaves of plants, blood plasma, muscle tissue, cells etc.) are light-scattering. Therefore, the directed beam of radiation after interaction with the object scatters in all directions (within 4π). We can gather with a special photometric device in a cavity field, the inner surface of which is covered with a layer of white, diffuse scattered paint (or material) based on powder MgO, $BaSO_4$.

The essence of spectrophotometric measurements is determined by the spectral dependence of optical properties of objects: reflection coefficient K, transmittance τ, absorption A. Measurement of these quantities for a fixed wavelength consists of two parts: the first measured value falling on the object spectral flow $F_{0\lambda}$, and then measured the value of flux reflected object $F_{k,\lambda}$ and missed him $F_{\tau,\lambda}$. Then, by definition, given parameters can be determined from the formulae

$$K_\lambda = \frac{\Phi_{K,\lambda}}{\Phi_{0\lambda}};\ \ \tau_\lambda = \frac{\Phi_{\tau,\lambda}}{\Phi_{0\lambda}}.\ ;\quad A_\lambda = 1-(K_\lambda + \tau_\lambda). \tag{2}$$

To study the linear dichroism, measurements of transmittance in polarized light at different orientations of the polarization plane relative to the direction of the dominant orientation in the structure of the sample of biological tissues were carried. The sample is centered in photometric sphere.

The technique of differential diagnosis of malignant or benign tumors using a simple optical method [8, 9] rather than sophisticated biochemical analysis is presented in this section. It isn't neccessary to measure across the whole spectrum, but rather to measure the magnitude of dichroic ratio, $D = \frac{1-\tau_0}{1-\tau_{90}}$, only at two characteristic wavelengths: λ_1 – in the maximum of the spectral dependence of Δ, and at λ_2 = 700–800 nm, for which Δ = 0. Their magnitudes for both types of tumors are present in Table 3 for the case of prostate cancer and in Table 4 – for the case of esophagus. It is seen that the dichroic ratio magnitudes for malignant tumors for both wavelengths differ in 1.5÷2.0 times for the case of prostate cancer, and up to 6–10% for esophagus, while benign or healthy tissue is virtually indistinguishable.

Table 3

Dichroic ratio for prostate cancer

№ of samples	Type of tumor	D, λ = 410 nm	D, λ = 800 nm
№ 1	Malignant	2,0	0,966
№ 2	Malignant	1,59	1,01
№ 3	Malignant	1,45	1,01
№ 4	Benign	1,099	1,013
№ 5	Benign	1,053	0,99
№ 6	Benign	1,042	1,007

Table 4

Dichroic ratio for esophageal tissues

№ of samples	Type of epithelium	D, λ = 440 nm	D, λ = 800 nm
№ 7	Malignant tumor	1,062	1,0
№ 8	Malignant tumor	1,085	1,0
№ 9	Healthy	1,00	1,009
№ 10	Healthy	1,006	1,0
№ 11	Healthy	1,00	1,0

The results of study of tumor tissue in the form of the spectral dependences of Δ for three samples are shown in Fig.7. It is seen that in domains λ < 320 nm and λ > 740-800 nm linear dichroism is practically absent, the maximal magnitude of Δ occurs at λ = 410 nm, while in contrast to aminoacids and proteins, these magnitudes are much larger and located within 8 to 22% depending on the individual characteristics of the patient.

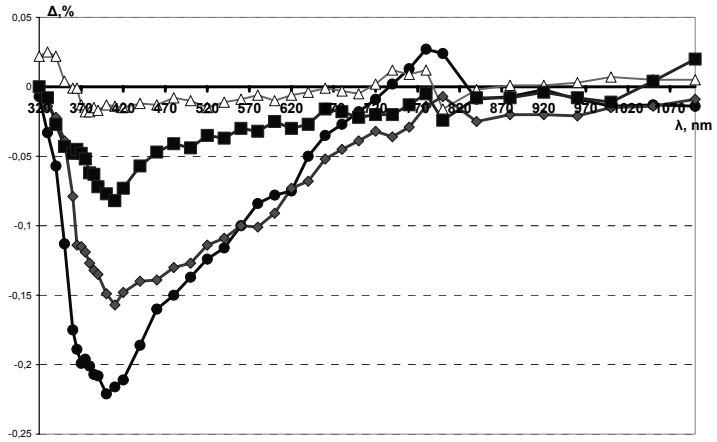

Fig. 7 – Spectral dependence of the linear dichroism of the prostate.

In order to investigate thin tissue cuts of the prostate gland, about one hundred cuts were produced. Unfortunately, the investigation was possible only on some of those cuts, as great amount of samples turned to be so small that the cutover of the beam exceeded their magnitudes. Despite this, the results of the investigation on different types of tumors (4–5 samples for each type) can be regarded as those that have general character [10–16].

The results of the investigation of the benign tumor tissues have showed that the magnitude of linear dichroism Δ is insignificant over whole spectral range λ = 280–840 nm, and specific regularities in its change aren't observed.

In Fig. 8, the spectral dependences of the dichroism magnitude for two tissue samples of the esophagus with a malignant tumor are showed, where one can see that within the domains λ < 380 nm and λ > 700 nm the linear dichroism also lacks. Two maxima are observed: at λ = 440 nm and λ ≈ 530–540 nm, and the last one is not clearly marked.

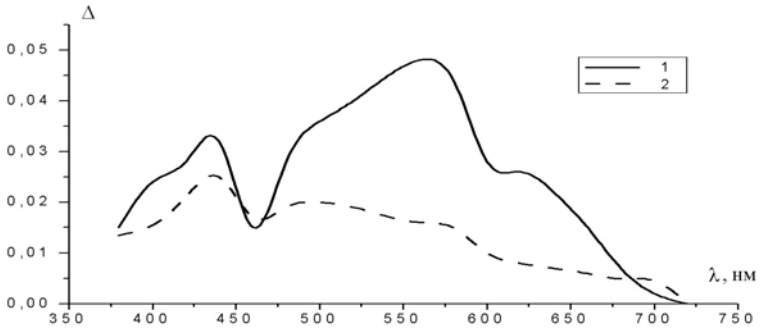

Fig. 8 – Spectral dependence of magnitude of the linear dichroism of the esophagus tissues:
1 – samples № 5, 2 – sample № 4.

The modelling of the cancer process in rats made it possible to trace how linear dichroism in muscle tissue with malignant tumors is developed in it. The results of study on the example of one of the rats are shown in Fig. 9. It is seen that the development of cancer of the linear dichroism increases, especially in the highs after 17 days of the lesions observed at $\lambda = 370$ nm and $\lambda = 460$ nm. In particular $\Delta = 0$ at $\lambda > 500$ nm. For a healthy tissue, linear dichroism is zero ($\Delta = 0$) within the whole investigated spectral domain.

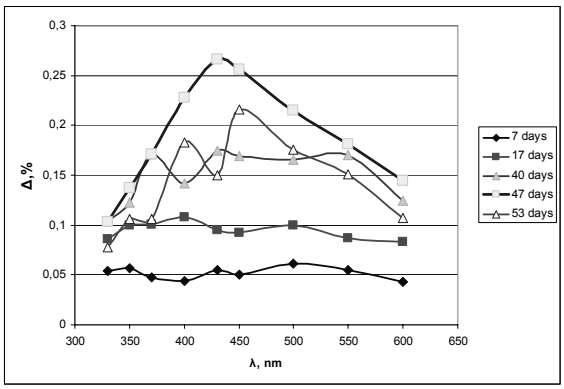

Fig. 9 – Spectral dependence of the linear dichroism of rat muscle tissue.

It should be noted that the study of linear dichroism by measuring transmittance of photometric area has the disadvantage that it is necessary to consider diffusely scattered radiation on the samples because they are optically homogeneous, which greatly complicates such studies. Therefore, we used the method of research on transmission [17]. The results of study of linear dichroism in cross-section sample of rat muscle tumor are shown in Fig. 10.

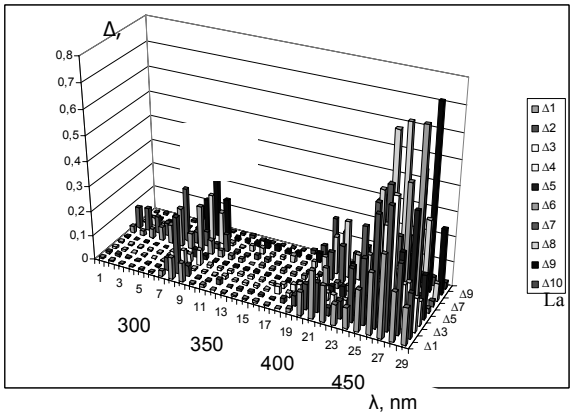

Fig.10 – Linear dichroism in cross cut rat muscle tumors.

There are two specific domains of the spectrum sensitive to cancer changes in tissues, one 320÷350 nm, which is caused by the emergence of concentration in the tumor fluorofor NADH, and 430÷470 nm area, which is caused by considerable growth of collagen (another fluorofor) in the tumor. The graph of tumor extent modeled 10^{th} layers of thin slices, the results of the obtained absorption bands coincide with the data of other literary sources [18].

5. CONCLUSIONS

The following conclusions can be made on the results of this investigation:

– an alternative approach (to biochemical one) for detecting cancer changes in biological tissues, which includes a simple technique of spectropolarimetry is offered to obtain magnitude of linear dichroism in tumor,

– spectral fingerprints manifestation of cancer changes in biological tissues is set,

– an attempt to establish substances in the tumor, which acts as optical indicators of cancer changes in biological tissues, has been done.

Acknowledgments. This work was supported by grant F53/103-2013 from the Fundamental Researches State Fund of Ukraine.

REFERENCES

1. H.S. Basaga, Biochem. and Cell Biol., **68**, *7–8*, 989–998 (1990).
2. A. Tkac, L. Bahna, Neoplasma, **29**, 497–516 (1982).
3. C.E. Cross, B. Halliwell, E.T. Borisch, Ann.Int.Med., **107**, 526–545 (1987).
4. G. Cao, R.L. Prior, Clin. Chem., **44**, 1309 (1998).
5. R. Kandar, V. Muzakova, A. Cegan, Clin.Chem.Lab.Med., **40**, 1032 (2002).
6. M.I. Gruia, R. Olinescu, M. Marinescu, I. Gruia, Rom.J.Comp.Onc.,**4**, 268 (2001).
7. O.V. Angelsky, S.B. Yermolenko, O.G. Prydij, J. Hol. Spec., **3**, 27–34 (2006).
8. A. Ushenko, S. Yermolenko, A. Prydij, S. Guminetsky, I. Gruia, O. Toma, K. Vladychenko, Proc. SPIE, **7008**, 70082C-1 - 70082C-11 (2008).
9. S. Yermolenko, A. Prydij, K. Vladychenko, Proc.SPIE, **7008**, 70082D-1-70082D-7 (2008).
10. O.V. Angelsky, P.P. Maksimyak, T.O. Perun, Appl. Opt., **32**, *30*, 6066–6071 (1993).
11. O.V. Angel'skii, A.G. Ushenko, A.D. Arkhelyuk, S.B. Ermolenko, Opt. i Spectr., **89**, *6*, 1050–1055, (2000).
12. O.V. Angel'skiĭ, A.G. Ushenko, A.D. Arkhelyuk, S.B. Ermolenko, Opt.i Spectr., **88**, *3*, 495–498, (2000).
13. O.V. Angelsky, A.Ya. Bekshaev, P.P. Maksimyak, A.P. Maksimyak, S.G. Hanson, C.Yu. Zenkova, Opt. Exp., **20**, *4*, 3563–3571 (2012).
14. O.V. Angelsky, A.Ya. Bekshaev, P.P. Maksimyak, A.P. Maksimyak, I.I. Mokhun, S.G. Hanson, C.Yu. Zenkova, A.V. Tyurin, Opt. Exp., **20**, *10*, 11351–11356 (2012).
15. A.Y. Bekshaev, O.V. Angelsky, S.G. Hanson, C.Y. Zenkova, Phys.Rev.A, **86**, 023847 (2012).
16. O.V. Angelsky, A.Ya. Bekshaev, P.P. Maksimyak, A.P. Maksimyak, S.G. Hanson, C.Yu. Zenkova, Opt. Exp., **21**, *7*, 8922–8938 (2013).

17. O.V. Angelsky, S.B. Yermolenko, C.Yu.Zenkova, A.O. Angelskaya, Appl. Opt., **47**, 5492–5499 (2008).
18. I. Gruia, S. Yermolenko, M. Gruia, P. Ivashko, T. Stefanescu, Optoel. and Adv. Mater.–Rap. Comm., **4**, *4*, 523–526 (2010).